

This article was downloaded by:

On: 25 January 2011

Access details: *Access Details: Free Access*

Publisher *Taylor & Francis*

Informa Ltd Registered in England and Wales Registered Number: 1072954 Registered office: Mortimer House, 37-41 Mortimer Street, London W1T 3JH, UK



## Liquid Crystals

Publication details, including instructions for authors and subscription information:

<http://www.informaworld.com/smpp/title~content=t713926090>

### Theoretical analysis of texture dependent extensional viscosity of discotic mesophases

Arvinder P. Singh; Alejandro D. Rey

Online publication date: 06 August 2010

**To cite this Article** Singh, Arvinder P. and Rey, Alejandro D.(1999) 'Theoretical analysis of texture dependent extensional viscosity of discotic mesophases', *Liquid Crystals*, 26: 6, 825 – 833

**To link to this Article:** DOI: 10.1080/026782999204516

**URL:** <http://dx.doi.org/10.1080/026782999204516>

PLEASE SCROLL DOWN FOR ARTICLE

Full terms and conditions of use: <http://www.informaworld.com/terms-and-conditions-of-access.pdf>

This article may be used for research, teaching and private study purposes. Any substantial or systematic reproduction, re-distribution, re-selling, loan or sub-licensing, systematic supply or distribution in any form to anyone is expressly forbidden.

The publisher does not give any warranty express or implied or make any representation that the contents will be complete or accurate or up to date. The accuracy of any instructions, formulae and drug doses should be independently verified with primary sources. The publisher shall not be liable for any loss, actions, claims, proceedings, demand or costs or damages whatsoever or howsoever caused arising directly or indirectly in connection with or arising out of the use of this material.

# Theoretical analysis of texture dependent extensional viscosity of discotic mesophases

ARVINDER P. SINGH and ALEJANDRO D. REY\*

Department of Chemical Engineering, McGill University, 3610 University Street,  
Montreal, Quebec H3A 2B2, Canada

(Received 26 August 1998; in final form 24 November 1998; accepted 1 December 1998)

Rheological functions for uniaxial extensional flows predicted by a previously selected and validated constitutive equation (CE) for discotic mesophases are presented. The predicted relations between extensional viscosities, flow-induced microstructure, processing conditions, and material parameters of discotic mesophases are characterized and discussed. It is found that, in contrast to rod-like nematics, two distinct uniaxial extensional viscosities need to be defined to characterize the extensional rheological functions of discotic mesophases completely. The model predicts non-Troutonian extensional viscosities of discotic nematics, such as strain thinning and strain thickening, depending on the process temperature, and the ratio of viscous to elastic stress contributions. The uniaxial extensional viscosities are also found to depend strongly on the flow-induced microstructure. The rheological analysis is then used to characterize the relations between extensional flow viscosities and the classical microstructures that arise during the industrial fiber spinning of discotic mesophase pitches.

## 1. Introduction

Mesophase pitches are used in the manufacture of high performance carbon fibres [1–7]. These fibres possess superior mechanical and thermal transport properties and find uses in a wide variety of applications ranging from space to the electronics industry [1]. A conventional high speed melt spinning process is employed in which the mesophase pitch is melted and then extruded through spinneret capillaries to form fibres which are subsequently drawn in the spin-line to accentuate the axial orientation [3–7]. Since the mesophase pitches have finite memory, the relative intensity of the various process steps and their sequence (i.e. conical section → capillary → die exit → spin-line) have a profound effect on the final microstructure of the carbon fibers. Also, spinning temperature is reported to have a significant effect on the selection of fibre texture [1]. The spinning process inherently involves extensional flows both inside the spin-pack and in the spin-line, therefore it is important to understand the behaviour of mesophase pitches under these flows [1–7]. In addition, the molecular orientation of discotic mesophases in the spin-line gives rise to characteristic textures, such as radial and onion [1], and the relation between extensional viscosities and fibre textures has not yet been characterized. This paper presents for the first time the theory

and simulation of uniaxial extensional viscosities of discotic mesophases, based on a validated tensorial model, and their relationships with flow-induced microstructure, processing conditions, and molecular geometry corresponding to those of carbonaceous mesophase pitches.

Mesophase pitches consist of flat, disk-like, aromatic molecules that tend to adopt a uniaxial discotic nematic phase  $N_D$ , with unit normals to the disc-like molecules more or less aligned along a common direction (see figure 1) represented by the uniaxial director  $\mathbf{n}$ ; in what follows we use  $\mathbf{n}$  and uniaxial orientation interchangeably. The degree of alignment of the unit normals along  $\mathbf{n}$  is given by the scalar order parameter  $S$ ; in what follows we use  $S$  and uniaxial alignment interchangeably. The flow-induced biaxiality in discotic mesophases is

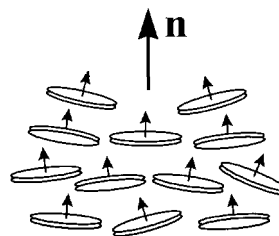


Figure 1. The uniaxial director orientation  $\mathbf{n}$  of uniaxial discotic nematic liquid crystals. The director  $\mathbf{n}$  is the average orientation of the unit normals to the disc-like molecules.

\* Author for correspondence; e-mail: alex@chemeng.lan.mcgill.ca

characterized in terms of biaxial directors/orientation  $\mathbf{m}$  and  $\mathbf{l}$ , and the biaxial scalar order parameter or alignment  $P$ ; details are given in [8].

It is well known that extensional flows are strongly orienting flows [8–10]. The basic flow orienting phenomena of nematics in extensional flows depend on the molecular geometry due to the fact that discotic (rod-like) nematics orient their shortest (longest) direction along the director  $\mathbf{n}$ . For discotic nematics the tumbling function or the reactive parameter is negative,  $\lambda < 0$ , and uniaxial extensional flows orient the uniaxial director  $\mathbf{n}$  anywhere in the compression plane, normal to the extension axis [8–10]. This flow-induced orientation naturally induces biaxiality [8] since the major axis (extension direction) of the rate-of-strain tensor ellipsoid is perpendicular to the main axis ( $\mathbf{n}$ ) of the tensor order parameter ellipsoid. On the other hand, for rod-like nematics the reactive parameter is positive,  $\lambda > 0$ ,  $\mathbf{n}$  aligns along the extension direction and the tensor order parameter is uniaxial.

The main purpose of this paper is to present the extensional rheological properties of discotic mesophases. The particular objectives of the paper are to:

- (1) Identify the important extensional rheological parameters for discotic mesophases;
- (2) Characterize the dependence of rheological material properties of discotic mesophases on their extensional flow-induced microstructure;
- (3) Establish the relationships between extensional rheological functions, flow-induced microstructure, processing conditions, and molecular geometry.

Although numerical predictions of this paper have not been directly validated due to the lack of available experimental data, yet a high degree of confidence can be expected since: (1) the present model has been shown to embrace the distinctive and experimentally observed shear-induced microstructure modes [4] and flow instability of discotic mesophases [7]; (2) the model presented in this paper has been shown to capture all the complex non-linear rheological phenomena actually exhibited by discotic as well as rod-like nematics [4, 7]. This paper is a continuation of our effort to increase the understanding of the rheology of discotic mesophases, and to provide theoretical guidelines for experimental work being pursued to understand the microstructure–processing–product property relationships in developing new high performance engineering materials.

The organization of this paper is as follows. The next section presents the theory, the coordinate system and kinematics along with the microstructure-governing CE and stress tensor equation. In §3 we present, discuss, and characterize the uniaxial extensional viscosity of discotic mesophases. The relationships between extensional

viscosity, microstructure, processing conditions, and materials parameters are also given. Finally, conclusions are presented. The appendix contains a brief analysis, based on Leslie–Ericksen (L–E) theory, of extensional viscosity of rod-like and discotic nematics.

## 2. Theory and governing equations

### 2.1. Definition of microstructure, kinematics and coordinates

In tensor theories the complete description of the microstructure of liquid crystalline materials is conveniently given by a symmetric and traceless second order tensor, generally known as tensor order parameter  $\mathbf{Q}$ , given in principal form as:

$$\mathbf{Q} = \lambda_n \mathbf{nn} + \lambda_m \mathbf{mm} + \lambda_l \mathbf{ll} \quad (1a)$$

where

$$\lambda_n = \frac{2}{3}S, \quad \lambda_m = -\frac{1}{3}(S - P), \quad \lambda_l = -\frac{1}{3}(S + P),$$

$$\text{and } -\frac{1}{3} \leq \lambda_a \leq \frac{2}{3}. \quad (1b, c, d, e)$$

The eigenvalues  $\lambda_a$  ( $\mathbf{a} = \mathbf{n}, \mathbf{m}, \mathbf{l}$ ) correspond to the unit eigenvectors ( $\mathbf{n}, \mathbf{m}, \mathbf{l}$ ) respectively, the latter forming a right handed orthogonal triad. The orientation is completely defined by the director triad ( $\mathbf{n}, \mathbf{m}, \mathbf{l}$ ). The magnitude of uniaxial alignment  $S = 3/2 \mathbf{n} \cdot \mathbf{Q} \cdot \mathbf{n}$  is a measure of molecular alignment along the uniaxial director  $\mathbf{n}$  and that of the biaxial alignment  $P = 3/2 \mathbf{m} \cdot \mathbf{Q} \cdot \mathbf{m} - 3/2 \mathbf{l} \cdot \mathbf{Q} \cdot \mathbf{l}$  is a measure of molecular alignment in a plane perpendicular to uniaxial director  $\mathbf{n}$ . Details on uniaxial ( $S$ ) and biaxial ( $P$ ) alignments and their interrelations are given in [8]. The present work is restricted to normal nematics ( $0 \leq S \leq 1$ ,  $0 \leq P \leq 1$ ). The order parameter  $\mathbf{Q}$  is assumed to be spatially uniform and Frank elasticity is not considered.

Figure 2 shows the deformations of an element of discotic mesophase subjected at time  $t = 0$  to a uniaxial extensional flow of constant extension rate  $\dot{\epsilon}$ . As shown, the extension direction is along the  $z$ -axis and  $r - \theta$  is the compression plane. The velocity field for the considered flow field is given as:

$$v_r = -\frac{1}{2}\dot{\epsilon}rH(t), \quad v_\theta = 0, \quad v_z = \dot{\epsilon}zH(t)$$

$$\text{where } H(t) = \begin{cases} 0 & t < 0 \\ 1 & t \geq 0 \end{cases}. \quad (2a, b, c, d)$$

In this paper we use the velocity field given by equation (2) and perform only a steady state analysis, i.e.  $t \rightarrow +\infty$ .

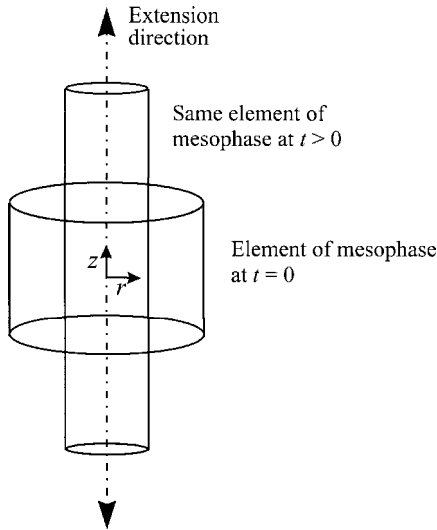


Figure 2. Deformation of a unit cylinder of discotic mesophase subjected at time  $t=0$  to a uniaxial extensional flow deformation. The extension direction is along the  $z$ -axis, and the  $r-\theta$  plane contains the uniform compression.

## 2.2. Microstructure constitutive equation for nematics

The microstructure response of liquid crystalline polymers, as described by Doi's mesoscopic nematodynamic theory [11], is given as:

$$\hat{\mathbf{Q}} = \mathbf{F}(\mathbf{Q}, \nabla \mathbf{v}) + \mathbf{H}(\mathbf{Q}, \bar{D}_r(\mathbf{Q})) \quad (3)$$

where  $\nabla \mathbf{v}$  is the velocity gradient tensor and  $\hat{\mathbf{Q}}$  is the corotational derivative of  $\mathbf{Q}$  and is defined as:

$$\hat{\mathbf{Q}} = \frac{\partial \mathbf{Q}}{\partial t} + (\mathbf{v} \cdot \nabla) \mathbf{Q} - \mathbf{W} \cdot \mathbf{Q} + \mathbf{Q} \cdot \mathbf{W}. \quad (4)$$

$\mathbf{F}(\mathbf{Q}, \nabla \mathbf{v})$  and  $\mathbf{H}(\mathbf{Q}, \bar{D}_r(\mathbf{Q}))$  represent the flow and the short range elastic contributions respectively, and are given as [12]:

$$\begin{aligned} \mathbf{F}(\mathbf{Q}, \nabla \mathbf{v}) = & \frac{2}{3} \beta \mathbf{A} + \beta \left[ \mathbf{A} \cdot \mathbf{Q} + \mathbf{Q} \cdot \mathbf{A} - \frac{2}{3} (\mathbf{A} : \mathbf{Q}) \delta \right] \\ & - \frac{1}{2} \beta [(\mathbf{A} : \mathbf{Q}) \mathbf{Q} + \mathbf{A} \cdot \mathbf{Q} \cdot \mathbf{Q} + \mathbf{Q} \cdot \mathbf{A} \cdot \mathbf{Q} \\ & + \mathbf{Q} \cdot \mathbf{Q} \cdot \mathbf{A} - \{(\mathbf{Q} \cdot \mathbf{Q}) : \mathbf{A}\} \delta] \end{aligned} \quad (5)$$

$$\begin{aligned} \mathbf{H}(\mathbf{Q}, \bar{D}_r(\mathbf{Q})) = & -6\bar{D}_r \left[ \left(1 - \frac{1}{3} U\right) \mathbf{Q} - U \mathbf{Q} \cdot \mathbf{Q} \right. \\ & \left. + U \left\{ (\mathbf{Q} : \mathbf{Q}) \mathbf{Q} + \frac{1}{3} (\mathbf{Q} : \mathbf{Q}) \delta \right\} \right] \end{aligned} \quad (6)$$

where

$$\bar{D}_r = D_r \left[ 1 - \frac{3}{2} (\mathbf{Q} : \mathbf{Q}) \right]^2, \quad \beta = \frac{p^2 - 1}{p^2 + 1}, \quad p = \frac{r_{\perp}}{r_{\parallel}}. \quad (7a, b, c)$$

Here  $\bar{D}_r$  is the averaged diffusivity,  $D_r$  is the pre-averaged diffusivity or rotary diffusivity of a hypothetical isotropic fluid under the same conditions,  $U$  ( $\propto 1/T$ ,  $T$  temperature) is the nematic potential, and  $\beta$  is the shape factor. To specify the molecular geometry we approximate the disk-like molecular shape of discotic mesophases with an oblate spheroid of aspect ratio  $p$  ( $p < 1$ ) where  $r_{\parallel}$  is the length of the shortest and distinct semiaxis, and  $r_{\perp}$  the length of the two longest and equal semiaxes. For an ideal flat disc  $p = 0$  ( $\beta = -1$ ), for a sphere  $p = 1$  ( $\beta = 0$ ), and for an infinitely long rod  $p \rightarrow \infty$  ( $\beta = 1$ ). For discotics ( $-1 < \beta < 0$ ); as  $\beta$  increases, the constituting aromatic disk-like molecules tend to become thicker.  $\mathbf{A}$  and  $\mathbf{W}$  are the rate of deformation and vorticity tensor respectively. For uniaxial extensional flows the vorticity tensor  $\mathbf{W}$  is zero, and  $\mathbf{A}$  is calculated using equations (2).

## 2.3. Symmetric visco-elastic stress tensor for nematics

The symmetric extra stress tensor  $\mathbf{t}^s$  for thermotropic liquid crystalline materials is expressed as a sum of viscous  $\mathbf{t}^v$  and elastic  $\mathbf{t}^e$  stress contributions [11, 13, 14] as:

$$\mathbf{t}^s = \mathbf{t}^v + \mathbf{t}^e. \quad (8)$$

The expression for the elastic stress contribution  $\mathbf{t}^e$ , derived by using the standard equation of fluxes ( $\mathbf{t}^s$ ,  $\hat{\mathbf{Q}}$ ) in terms of forces ( $\mathbf{A}$ ,  $\mathbf{H}$ ) [13, 15, 16], for the presented CE, equation (3) is:

$$\begin{aligned} \mathbf{t}^e = (c\kappa T) \left[ -\frac{2}{3} \beta \mathbf{H} - \beta \left\{ \mathbf{H} \cdot \mathbf{Q} + \mathbf{Q} \cdot \mathbf{H} - \frac{2}{3} (\mathbf{H} : \mathbf{Q}) \delta \right\} \right. \\ \left. + \frac{1}{2} \beta \{ (\mathbf{H} : \mathbf{Q}) \mathbf{Q} + \mathbf{H} \cdot \mathbf{Q} \cdot \mathbf{Q} + \mathbf{Q} \cdot \mathbf{H} \cdot \mathbf{Q} \right. \\ \left. + \mathbf{Q} \cdot \mathbf{Q} \cdot \mathbf{H} - ((\mathbf{Q} \cdot \mathbf{Q}) : \mathbf{H}) \delta \} \right] \end{aligned} \quad (9)$$

where

$$\begin{aligned} \mathbf{H}(\mathbf{Q}) = \frac{1}{6\bar{D}_r} \mathbf{H}(\mathbf{Q}, \bar{D}_r(\mathbf{Q})) = - \left[ \left(1 - \frac{1}{3} U\right) \mathbf{Q} - U \mathbf{Q} \cdot \mathbf{Q} \right. \\ \left. + U \left\{ (\mathbf{Q} : \mathbf{Q}) \mathbf{Q} + \frac{1}{3} (\mathbf{Q} : \mathbf{Q}) \delta \right\} \right] \end{aligned} \quad (10)$$

and  $c$  is the number of molecules per unit volume,  $\kappa$  the Boltzmann constant and  $T$  the absolute temperature. The viscous stress contribution  $\mathbf{t}^v$  is given by:

$$\begin{aligned} \mathbf{t}^v = \Xi : \mathbf{A} = v_1 \mathbf{A} + v_2 \left[ \mathbf{Q} \cdot \mathbf{A} + \mathbf{A} \cdot \mathbf{Q} - \frac{2}{3} (\mathbf{Q} : \mathbf{A}) \delta \right] \\ + v_3 [(\mathbf{A} : \mathbf{Q}) \mathbf{Q} + \mathbf{A} \cdot \mathbf{Q} \cdot \mathbf{Q} + \mathbf{Q} \cdot \mathbf{A} \cdot \mathbf{Q} \\ + \mathbf{Q} \cdot \mathbf{Q} \cdot \mathbf{A} + ((\mathbf{Q} \cdot \mathbf{Q}) : \mathbf{A}) \delta] \end{aligned} \quad (11)$$

where  $\Xi$  is the fourth order tensor, and  $\nu_1$ ,  $\nu_2$  and  $\nu_3$  are viscosity coefficients. Mapping the above expression to those given in [11, 14], in which the viscous contribution to the stress tensor contains contributions from  $\mathbf{Q}^2$  terms only, we arrive at:

$$\mathbf{t}^v = \mu [(\mathbf{A} : \mathbf{Q})\mathbf{Q} + \mathbf{A} \mathbf{Q} \mathbf{Q} + \mathbf{Q} \mathbf{A} \mathbf{Q} + \mathbf{Q} \mathbf{Q} \mathbf{A} + ((\mathbf{Q} \mathbf{Q}) : \mathbf{A})\delta] \quad (12)$$

where  $\nu_1 = \nu_2 = 0$  and  $\nu_3 = \mu$ . Combining equations (9) and (12), the dimensionless symmetric extra stress tensor  $\tilde{\mathbf{t}}^s$  is given by [16]:

$$\begin{aligned} \tilde{\mathbf{t}}^s = \frac{\mathbf{t}^s}{c\kappa T} = & \xi_v De [(\tilde{\mathbf{A}} : \mathbf{Q})\mathbf{Q} + \tilde{\mathbf{A}} \mathbf{Q} \mathbf{Q} + \mathbf{Q} \tilde{\mathbf{A}} \mathbf{Q} \\ & + \mathbf{Q} \mathbf{Q} \tilde{\mathbf{A}} - ((\mathbf{Q} \mathbf{Q}) : \tilde{\mathbf{A}})\delta] \\ & + \beta \left[ -\frac{2}{3}\mathbf{H} - \left\{ \mathbf{H} \mathbf{Q} + \mathbf{Q} \mathbf{H} - \frac{2}{3}(\mathbf{H} : \mathbf{Q})\delta \right\} \right. \\ & + \frac{1}{2} \{ (\mathbf{H} : \mathbf{Q})\mathbf{Q} + \mathbf{H} \mathbf{Q} \mathbf{Q} + \mathbf{Q} \mathbf{H} \mathbf{Q} + \mathbf{Q} \mathbf{Q} \mathbf{H} \\ & \left. - ((\mathbf{Q} \mathbf{Q}) : \mathbf{H})\delta \right] \quad (13) \end{aligned}$$

where  $\xi_v = \mu 6D_r / c\kappa T$  is a dimensionless constant representing the ratio of the viscous  $\mathbf{t}^v$  to the elastic  $\mathbf{t}^e$  stress contributions, previously introduced by Larson [14];  $De = \dot{\epsilon} / 6D_r$  is the Deborah number or the dimensionless strain rate,  $\tilde{\mathbf{A}}$  ( $\tilde{\mathbf{A}} = \mathbf{A} / \dot{\epsilon}$ ) is the dimensionless rate of strain tensor, and  $\dot{\epsilon}$  is the extension rate.

#### 2.4. Uniaxial extensional viscosities of discotic nematics

The classical definition of uniaxial extensional viscosity for isotropic materials, also referred to as elongational viscosity or tensile viscosity, is given by [17]:

$$\eta_E(\dot{\epsilon}) = \lim_{t \rightarrow \infty} \left[ \frac{\sigma_E(t, \dot{\epsilon})}{\dot{\epsilon}} \right] \quad (14)$$

where  $\sigma_E = t_{zz}^s - t_{rr}^s$  is the tensile modulus. However, for discotic nematic liquid crystals the above definition is incomplete because there are two different extensional viscosities, as explained below and shown in Appendix A. These two extensional viscosities are defined as follows:

$$\eta_{zr} = \frac{t_{zz}^s - t_{rr}^s}{\dot{\epsilon}}, \quad \eta_{z\theta} = \frac{t_{zz}^s - t_{\theta\theta}^s}{\dot{\epsilon}} \quad (15a, b)$$

and in dimensionless form

$$\begin{aligned} \eta_{zi}^* = \frac{\eta_{zi}}{(c\kappa T)De} = & \frac{6D_r}{c\kappa T} \frac{t_{zz}^s - t_{ii}^s}{\dot{\epsilon}} = \frac{\tilde{t}_{zz}^s - \tilde{t}_{ii}^s}{De} \\ & \text{where } i = r \text{ and } \theta. \quad (16) \end{aligned}$$

For simplicity, in what follows the superscript “\*” is dropped. It is important to note that for rod-like nematics

only one extensional viscosity is needed because  $\mathbf{n}$  orients along the extension direction ( $z$ -axis). On the other hand, in discotic nematics  $\mathbf{n}$  orients normal to the extension direction and anywhere in the compression plane ( $r - \theta$ ), so that the symmetry of the compression plane is broken, and therefore two viscosities are needed. In what follows we show the relations between the two extensional viscosities, equations (15), and the microstructures that arise in the spinning of carbonaceous mesophases [4].

### 3. Results and discussion

This section is subdivided into two. Section 3.1 discusses the microstructural features (orientation and alignment) of discotic mesophases subjected to uniaxial extensional flows needed to explain extensional flow rheology. Section 3.2 presents the extensional rheological properties of discotic mesophases.

#### 3.1. Orientation and alignment of discotic mesophases under extensional flows

The detailed dynamic analysis of the orientation director triad ( $\mathbf{n}, \mathbf{m}, \mathbf{l}$ ) and uniaxial  $S$  and biaxial  $P$  alignments of discotic mesophases under extensional flows are given in [8]. As mentioned above, here we study only the steady state rheological features of discotic mesophases under extensional flows. At steady state the uniaxial  $\mathbf{n}_{ss}$ , and biaxial  $\mathbf{m}_{ss}$  directors lie in the compression plane ( $r - \theta$  plane) whereas the biaxial director  $\mathbf{l}_{ss}$  lies along the extension direction ( $z$ -axis). The steady state orientation of the director triad ( $\mathbf{n}_{ss}, \mathbf{m}_{ss}, \mathbf{l}_{ss}$ ) is independent of extensional rate  $De$ , nematic potential  $U$ , and shape factor  $\beta$ . However, the dynamics of the orientation director triad are functions of these parameters [8–10].

In this work we have obtained the stable steady state solutions to equations (3) for a velocity field given by equations (2). The output consists of the components of the steady state tensor order parameter  $\mathbf{Q}_{ss}(De)$  which is transformed to principal form to determine its eigenvalues (to evaluate steady state alignments  $S_{ss}$  and  $P_{ss}$ ) and eigenvectors or steady state orientation triad ( $\mathbf{n}_{ss}, \mathbf{m}_{ss}, \mathbf{l}_{ss}$ ). The parametric study is performed by choosing two values, low and high, of the nematic potential  $U$  ( $U = 3, 6$ ), and the shape factor  $\beta$  ( $\beta = -0.8, -0.6$ ). In the present case, i.e. in the absence of spatial gradients, both  $S_{ss}$  and  $P_{ss}$  are independent of the steady state director triad orientation ( $\mathbf{n}_{ss}, \mathbf{m}_{ss}, \mathbf{l}_{ss}$ ). Figure 3 shows the steady state uniaxial  $S_{ss}$  and biaxial  $P_{ss}$  scalar order parameters as a function of  $De$  for  $U = 6$  (full line) and  $U = 3$  (dash-line), for  $\beta = -0.8$  (upper), and  $\beta = -0.6$  (lower).  $S_{ss}$  increases monotonically with the dimensionless strain rate  $De$  at all values of  $U$  and  $\beta$ .  $P_{ss}$  at higher  $U$  ( $U = 6$ ) follows the similar trend and increases monotonically with  $De$  for both values of  $\beta$ ; however

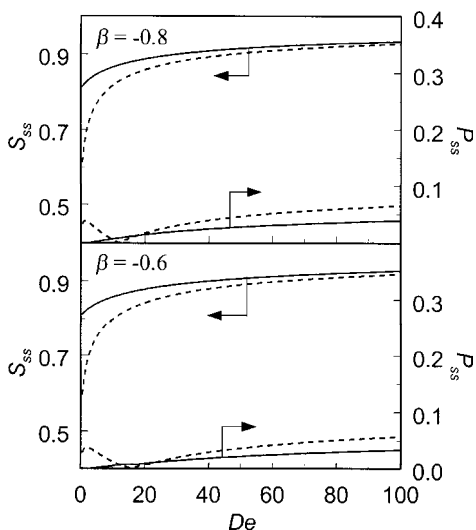


Figure 3. Steady state uniaxial  $S_{ss}$  and biaxial  $P_{ss}$  scalar order parameters as a function of  $De$  for  $U = 6$  (full line) and  $U = 3$  (dash-line), for  $\beta = -0.8$  (upper) and  $\beta = -0.6$  (lower).  $S_{ss}$  increases monotonically with the dimensionless strain rate  $De$  at all values of  $U$  and  $\beta$ .  $P_{ss}$  at higher  $U$  ( $U = 6$ ) follows a similar trend, however at lower  $U$  ( $U = 3$ ) there is a local minimum. Both  $S_{ss}$  and  $P_{ss}$  for discotic mesophases consisting of thicker molecules,  $\beta = -0.6$ , are less than those with relatively thinner molecules,  $\beta = -0.8$ .

at lower  $U$  ( $U = 3$ ) there is a local minimum for intermediate values of  $De$ , thereafter it increases monotonically with  $De$ . For discotic mesophases with a given shape factor  $\beta$ ,  $S_{ss}$  at high  $U$  is always greater than that at low  $U$ , however the difference  $\Delta S_{ss} (= S_{ss,highU} - S_{ss,lowU})$  between values at high and low  $U$  decreases with increasing  $De$ . On the other hand  $P_{ss}$  at high  $U$  is less than that at low  $U$ , and the difference  $\Delta P_{ss} (= P_{ss,lowU} - P_{ss,highU})$  increases with  $De$ . Both  $S_{ss}$  and  $P_{ss}$  for discotic mesophases consisting of thicker disks,  $\beta = -0.6$ , are less than those with the relatively thinner disks,  $\beta = -0.8$  for all  $U$  and  $De$ . Though not shown in figure 3, as  $De \rightarrow 0$ , uniaxiality is recovered, i.e.  $P_{ss} \rightarrow 0$ , for all values of nematic potential  $U$  ( $U = 6, 3$ ) and shape factor  $\beta$  ( $\beta = -0.6, -0.8$ ) considered here.

In this paper the spatial variation of order parameter is not considered when capturing the extensional viscosities corresponding to the characteristic textures of discotic mesophase fibres. As is well known [13], the intrinsic length scale of the model  $\zeta$ , where there are variations in order parameter, is given as:

$$\zeta = \left[ \frac{L}{(d^2 \Lambda_H / dS^2)_{S_B}} \right]^{1/2} \quad (17)$$

where  $L$  is the elastic constant,  $\Lambda_H$  is the homogeneous free energy density [18], and  $S_B$  is the bulk order parameter. For liquid crystal systems this correlation

length is less than  $10^{-2} \mu\text{m}$  and thus significantly smaller than the fibre radius ( $\sim 1 \mu\text{m}$ ), and to simplify the analysis we can assume as a first approximation that  $\nabla \lambda_i = 0$  ( $i = \mathbf{n}, \mathbf{m}, \mathbf{l}$ ). Therefore in what follows we use the homogeneous scalar order parameter (i.e.  $\nabla S = \nabla P = \mathbf{0}$ ) results obtained in this section to calculate extensional viscosities in the presence of the orientation gradients (i.e.  $\nabla \mathbf{n} \neq \mathbf{0}, \nabla \mathbf{m} \neq \mathbf{0}$ ) that arise in cylindrical coordinates (see figure 4).

### 3.2. Uniaxial extensional viscosity of discotic mesophases

This section presents the predicted extensional viscosity and its relationship with the flow-induced internal microstructure ( $\mathbf{Q}$ ), processing conditions ( $U \propto 1/T$ ), and material parameters ( $\beta$ ), of relevance to the industrial fibre spinning of mesophase pitches. It is well documented that during this process the fibre cross-section may exhibit the onion or radial textures [1] shown in figure 4. The figure shows schematics of the radial and onion microstructure mode with respect to the cylindrical coordinate system with the  $z$ -axis (extensional direction) perpendicular to the page. The dotted lines show the side view of the disk-like molecules, such that for radial (onion) mode, the unit normals to the disk-like molecules orient along the azimuthal  $\theta$  (radial  $r$ ) direction. These two modes also exist as the prevalent transverse fibre textures in mesophase carbon fibres [1]. To study the effect of processing conditions and material parameters, the same parametric values for  $U$  and  $\beta$ , as stated above, are used.

As shown in the Appendix the Leslie-Ericksen [19] theory for discotic mesophases indicates that two uniaxial extensional viscosities need to be defined to characterize their extensional rheological functions completely, in contrast to rod-like nematics which need only

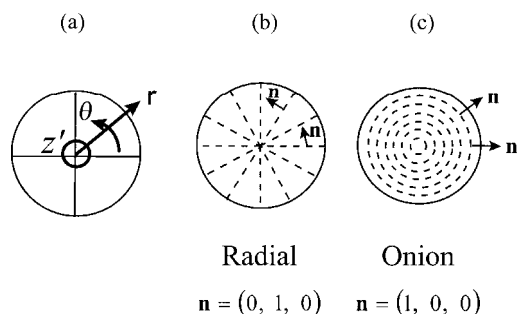


Figure 4. Schematics of (a) cylindrical coordinate system, and the two main representative mesophase pitch-based carbon fibre transverse textures: (b) radial, and (c) onion. In the radial (onion) texture, the unit normals to the disk-like molecules orient along the azimuthal  $\theta$  (radial  $r$ ) direction. These textures are observed in the spinning of carbonaceous mesophases [1].

one. Thus to characterize the extensional viscosities for discotic nematics with the two observed microstructures, radial and onion, we use the following nomenclature:

$$\eta_{zj}^i = \frac{t_{zz}^i - t_{jj}^i}{De} \quad (18)$$

where  $i=r, o$  represents the radial and onion texture respectively, and  $j=r, \theta$  represents the two axes in the cylindrical coordinate system, see figure 4(a). For example the two extensional viscosities corresponding to the radial texture are:  $\eta_{zr}^r$  and  $\eta_{z\theta}^r$ , the former is given as the ratio of the difference of the diagonal components of the extra stress tensor  $\mathbf{t}^s$  along  $z$  and  $r$  directions to the strain rate, and the latter by the ratio of the difference of the diagonal components of the extra stress tensor  $\mathbf{t}^s$  along  $z$  and  $\theta$  directions to the strain rate. In the present model, the extension viscosity is a function of flow-induced microstructure  $\mathbf{Q}$ , nematic potential  $U$ , strain rate  $De$  and the shape factor  $\beta$ , and can be represented by

$$\eta_{zj}^i = \Psi(\beta, U, De, \mathbf{Q}^i) \quad (19)$$

where the microstructure tensor  $\mathbf{Q}^i$  [ $i=r$  (radial),  $i=o$  (onion)] for radial ( $\mathbf{Q}^r$ ) and onion ( $\mathbf{Q}^o$ ) texture is given as:

$$\mathbf{Q}^r = \lambda_m \hat{\delta}_r \hat{\delta}_r + \lambda_n \hat{\delta}_\theta \hat{\delta}_\theta + \lambda k \hat{k} \hat{k} \quad (20)$$

$$\mathbf{Q}^o = \lambda_n \hat{\delta}_r \hat{\delta}_r + \lambda_m \hat{\delta}_\theta \hat{\delta}_\theta + \lambda k \hat{k} \hat{k} \quad (21)$$

where  $\hat{\delta}_r, \hat{\delta}_\theta$  and  $\hat{k}$  are the unit vectors along the three cylindrical coordinates; the superscript in  $\mathbf{Q}$  represents the texture:  $i=r$  (radial),  $i=o$  (onion).

Figure 5 shows the computed dimensionless uniaxial extensional viscosities  $\eta_{zr}^i$  and  $\eta_{z\theta}^i$  of a discotic mesophase as a function of  $De$  for  $\xi_v = 0.001$  (full line), 0.1 (dash line), and 0.2 (triple dot-dash line); for  $\beta = -0.8$  and  $U = 6$  (a, b), and  $U = 3$  (c, d). The extensional viscosity  $\eta_{zr}^i$  ( $\eta_{z\theta}^i$ ) for the radial mode  $\eta_{zr}^r$  ( $\eta_{z\theta}^r$ ) is always less (greater) than for the onion mode  $\eta_{zr}^o$  ( $\eta_{z\theta}^o$ ) i.e.  $\eta_{zr}^r < \eta_{zr}^o$  ( $\eta_{z\theta}^r > \eta_{z\theta}^o$ ), at all  $De$  for all values  $U$  and  $\beta$ . Please also note that  $\eta_{zr}^r = \eta_{z\theta}^o$  and  $\eta_{zr}^o = \eta_{z\theta}^r$ , therefore we have  $\eta_{zr}^r = \eta_{z\theta}^o < \eta_{zr}^o = \eta_{z\theta}^r$ . The dependence of uniaxial extensional viscosities,  $\eta_{zr}^i$  and  $\eta_{z\theta}^i$ , for the radial and the onion textures on  $U, \beta$  and  $De$  are summarized in the table. For high  $U$  ( $U = 6$ ),  $\eta_{zr}^i$  (each  $\eta_{zr}^r$  and  $\eta_{zr}^o$ ) is independent of low  $De$ , but exhibits slight strain thinning for  $\xi_v = 0.001$ , and strain thickening for  $\xi_v = 0.1$ , and 0.2 at high  $De$ . It is found that the strain thinning (thickening) is due to elastic (viscous) stress contribution, since as the viscous contribution to total stress increases, the discotic mesophases exhibit stronger strain thickening characteristics. This phenomenon is more apparent at low  $U$  (higher  $T$ ). As shown in the table,  $\eta_{zr}^r$  follows

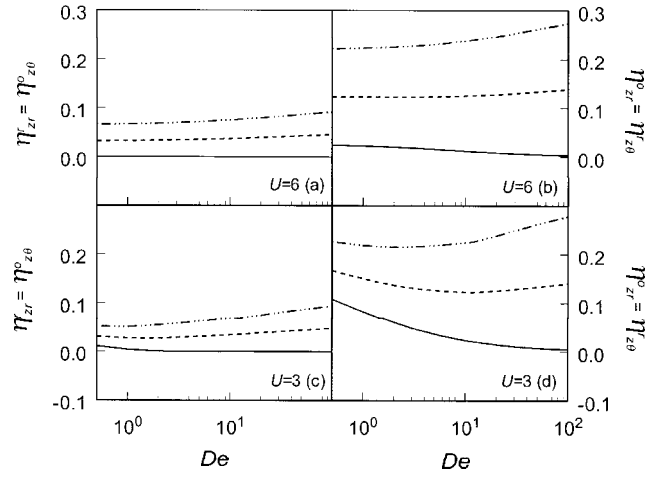


Figure 5. Dimensionless uniaxial extensional viscosities  $\eta_{zr}^i$  and  $\eta_{z\theta}^i$  [ $i=r$  (radial),  $i=o$  (onion)] of discotic mesophase as a function of  $De$  for  $\xi_v = 0.001$  (full line), 0.1 (dash line), and 0.2 (triple dot-dash line); for  $\beta = -0.8$  and  $U = 6$  (a, b), and  $U = 3$  (c, d). The extensional viscosity  $\eta_{zr}^i$  ( $\eta_{z\theta}^i$ ) for the radial texture  $\eta_{zr}^r$  ( $\eta_{z\theta}^r$ ) is always less (greater) than for the onion texture  $\eta_{zr}^o$  ( $\eta_{z\theta}^o$ ), i.e.  $\eta_{zr}^r < \eta_{zr}^o$  ( $\eta_{z\theta}^r > \eta_{z\theta}^o$ ). Also note that  $\eta_{zr}^r = \eta_{z\theta}^o$  and  $\eta_{zr}^o = \eta_{z\theta}^r$ , therefore  $\eta_{zr}^r = \eta_{z\theta}^o < \eta_{zr}^o = \eta_{z\theta}^r$  for details see text.

Table. Effect of processing conditions on uniaxial extensional viscosities of discotic mesophases ‘—’ strain rate independent viscosity, ‘↓’ strain thinning, ‘↑’ strain thickening,  $U$  nematic potential ( $\propto 1/T$ , temperature),  $\xi_v$  ratio of viscous to elastic stress contributions,  $De$  dimensionless strain rate,  $\eta_{zr}^r, \eta_{z\theta}^r, \eta_{zr}^o, \eta_{z\theta}^o$  dimensionless uniaxial extensional viscosities of discotic mesophases.

Parameter	Uniaxial extensional viscosities							
	6(high)				3(low)			
$\xi_v$	0.001		0.1, 0.2		0.001		0.1, 0.2	
$De$	low	high	low	high	low	high	low	high
$\eta_{zr}^r = \eta_{z\theta}^o$	—	↓	—	↑	—	↓	—	↑
$\eta_{zr}^o = \eta_{z\theta}^r$	—	↓	—	↑	↓	—	↓	↑

the same trend at low and high  $U$ . However, at low  $U$ ,  $\eta_{zr}^o$  exhibits strain thinning at low  $De$  with saturation at high  $De$  for  $\xi_v = 0.001$ , and strain thinning for low  $De$  and strain thickening at high  $De$ , with transition from thinning to thickening at intermediate  $De$ , for  $\xi_v = 0.1$  and 0.2. At low  $De$  the departure from equilibrium is higher at low  $U$  (see figure 4), thus elastic stress contributes more at low  $U$  and low  $De$ , thereby showing strain thinning at low strain rates, with strain thickening at high rates. Also, as elastic (viscous) stress dominates at low (high)  $De$ , therefore strain thinning (thickening) is seen at low (high) strain rates, with an intermediate  $De$

strain thinning → thickening transition, see figure 5(d) and the table). Though extensional viscosities at very low  $De$  are not presented here, at very low  $De$  ( $De \rightarrow 0$ ) the visco-elastic effects on microstructure and stress vanish and the viscosities are constant. The terminology for low/high  $De$  is used just to explain the most important results presented in figure 5.

Although not shown, the effect of the shape factor  $\beta$  on both of the extensional viscosities has been characterized. It is found that as  $\beta$  increases the extensional viscosities  $\eta_{zr}^i$  and  $\eta_{z\theta}^i$  decrease. For a fixed director triad orientation (radial or onion in the present case), the extensional viscosities are functions of the steady state eigenvalues ( $\lambda_n, \lambda_m, \lambda_l$ ) or the uniaxial  $S_{ss}$  and biaxial  $P_{ss}$  alignments; see equations (1, 19). As explained above and shown in figure 3, both  $S_{ss}$  and  $P_{ss}$  decrease with increasing  $\beta$ , hence  $\eta_{zr}^i$  and  $\eta_{z\theta}^i$  decrease with increasing  $\beta$ . All the above mentioned equalities, i.e.  $\eta_{zr}^r = \eta_{z\theta}^o$  and  $\eta_{zr}^o = \eta_{z\theta}^r$ , and inequalities, i.e.  $\eta_{zr}^r < \eta_{zr}^o$  and  $\eta_{z\theta}^r > \eta_{z\theta}^o$ , also follow at higher  $\beta$  ( $\beta = -0.6$ ).

The above discussed viscosity–microstructure relationships can be summarized as follows:

Inequalities within a given texture

$$\eta_{z\theta}^r > \eta_{zr}^r; \quad \eta_{zr}^o > \eta_{z\theta}^o \quad (22 a, b)$$

Equalities between two different textures

$$\eta_{z\theta}^r = \eta_{zr}^o; \quad \eta_{zr}^r = \eta_{z\theta}^o \quad (23 a, b)$$

To understand the above equalities and inequalities we use symmetry. The extensional viscosities for discotic mesophase depend on the microstructure  $\mathbf{Q}$ , the nematic potential  $U$ , the strain rate  $De$ , and the shape factor  $\beta$ :

$$\eta_{z\theta}^r = \Psi(\beta, U, De, \lambda_n, \lambda_l) \quad \text{and} \quad \eta_{zr}^o = \Psi(\beta, U, De, \lambda_n, \lambda_l) \quad (24 a, b)$$

where  $\lambda_n, \lambda_m, \lambda_l$  are the eigenvalues of  $\mathbf{Q}$ ; see equation (1). Since the eigenvalue  $\lambda_n$ , along  $\theta$  direction for the radial texture is equal to the eigenvalue  $\lambda_n$  along  $r$  for the onion texture, and since  $\lambda_l$  is common to both we find:

$$\eta_{z\theta}^r = \eta_{zr}^o. \quad (25)$$

Similarly

$$\eta_{zr}^r = \Psi(\beta, U, De, \lambda_m, \lambda_l) \quad \text{and} \quad \eta_{z\theta}^o = \Psi(\beta, U, De, \lambda_m, \lambda_l) \quad (26 a, b)$$

Since the eigenvalue  $\lambda_m$  along  $r$  direction for the radial texture is equal to the eigenvalue  $\lambda_m$  along  $\theta$  for the onion texture, and since  $\lambda_l$  is common to both we have:

$$\eta_{zr}^r = \eta_{z\theta}^o \quad (27)$$

Next, we will establish the origin of the inequalities (22) in the uniaxial extensional viscosities within a given texture. From equations (19–21), (24 a) and (26 a), and

since  $\lambda_n > \lambda_m$ , we have the inequality:

$$\eta_{z\theta}^r > \eta_{zr}^r. \quad (28)$$

Likewise from equations (19–21), (24 b) and (26 b), and with  $\lambda_n > \lambda_m$ , the second inequality follows:

$$\eta_{zr}^o > \eta_{z\theta}^o \quad (29)$$

We note that even in the uniaxial approximation ( $\lambda_n \neq \lambda_m = \lambda_l$ ), there will be two distinct extensional viscosities for discotic mesophases, and the inequalities between the uniaxial extensional viscosities for discotic mesophases presented above will hold. The Appendix shows that the texture dependent equalities and inequalities between the viscosity coefficients hold in the uniaxial limits also, using L–E theory.

#### 4. Conclusions

Predictions of uniaxial extensional rheological functions of discotic mesophases are presented and classified. The predicted rheological functions are discussed and assessed within the context of nematorheology.

For discotic mesophases two uniaxial extensional viscosities, termed here  $\eta_{zr}$  as and  $\eta_{z\theta}$  are needed to characterize completely their extensional rheological functions. The extensional viscosities depend strongly on the microstructure such that  $\eta_{zr}^r < \eta_{zr}^o$  and  $\eta_{z\theta}^r > \eta_{z\theta}^o$ . The extensional viscosities are different within a given texture, for example for radial (onion) texture  $\eta_{zr}^r < \eta_{z\theta}^r$  ( $\eta_{zr}^o > \eta_{z\theta}^o$ ). The discotic mesophases are found to be non-Troutonian, and show strain thinning or thickening based temperature and ratio of viscous to elastic stress contributions. The elastic (viscous) stresses result in strain thinning (thickening) characteristics of the discotic mesophases.

The microstructure dependency of the extensional viscosity of discotic mesophases has direct impact on the selection of the experimental technique for its measurement. The preferred microstructure (radial, onion, mixed radial onion, or folded) develops inside the spinneret capillaries, and the strong extensional flows accentuate the axial orientation of the molecules [3–7]. Thus if spinning devices are employed to measure the extensional viscosity, then prevailing microstructure in the thread-line needs to be specified along with the extensional viscosity data.

Acknowledgment is made to the Donors of The Petroleum Research Fund (PRF), administered by the American Chemical Society, for support of this research. The authors wish to thank Prof. D. D. Edie and Dr O. Fleurot for helpful discussion during the stay of APS at Clemson University.



### Appendix

#### Uniaxial extensional viscosity predictions from Leslie–Ericksen theory

The purpose of this appendix is to show, in the context of a vector theory (Leslie–Ericksen theory) [19] that two extensional viscosities need to be defined to characterize the uniaxial extensional functions of discotic nematics, whereas only one extensional viscosity coefficient is needed for rod-like nematics. Also ordering equalities and inequalities between uniaxial extensional viscosities, with regard to textures in discotic nematics, are also established using the L–E theory.

For anisotropic fluids, the stress tensor  $\tau$  as given by the L–E theory [19] is:

$$\tau = \alpha_1 \mathbf{A} : \mathbf{n} \mathbf{n} \mathbf{n} \mathbf{n} + \alpha_4 \mathbf{A} + \alpha_5 \mathbf{n} \mathbf{n} \cdot \mathbf{A} + \alpha_6 \mathbf{A} \cdot \mathbf{n} \mathbf{n} + \alpha_2 \mathbf{n} \mathbf{N} + \alpha_3 \mathbf{N} \mathbf{n} \quad (\text{A1})$$

where

$$\mathbf{N} = \dot{\mathbf{n}} - \mathbf{n} \cdot \mathbf{W}. \quad (\text{A2})$$

For extensional flows at steady state

$$\mathbf{W} = \mathbf{0}, \quad \dot{\mathbf{n}} = \mathbf{0}, \quad \therefore \mathbf{N} = \mathbf{0} \quad (\text{A3 } a, b)$$

and  $\mathbf{A}$  is given by equations (2). Equation (A1) for extensional flows and at steady state reduces to:

$$\tau = \alpha_1 \mathbf{A} : \mathbf{n} \mathbf{n} \mathbf{n} \mathbf{n} + \alpha_4 \mathbf{A} + \alpha_5 \mathbf{n} \mathbf{n} \cdot \mathbf{A} + \alpha_6 \mathbf{A} \cdot \mathbf{n} \mathbf{n}. \quad (\text{A4})$$

For rod-like nematics:

$$\mathbf{n}_{ss}(n_r, n_\theta, n_z) = (0, 0, 1). \quad (\text{A5})$$

The diagonal components of the stress tensor  $\tau$  are given as

$$\tau_{rr} = \tau_{\theta\theta} = -\frac{\dot{\epsilon}}{2} \alpha_4 \quad (\text{A5 } a, b)$$

$$\tau_{zz} = (\alpha_1 + \alpha_4 + \alpha_5 + \alpha_6) \dot{\epsilon} \quad (\text{A5 } c)$$

where  $\dot{\epsilon}$  is strain rate. As  $\tau_{rr} = \tau_{\theta\theta}$ , there is only one uniaxial extensional viscosity for rod-like nematics given as:

$$\eta_{\text{uni, rods}} = \frac{3}{2} \alpha_4 + \alpha_1 + \alpha_5 + \alpha_6. \quad (\text{A6})$$

Similarly, for discotic mesophases subjected to uniaxial/extensional flows [8–10]:

$$\mathbf{n}_{ss}(n_r, n_\theta, n_z) = (n_r, n_\theta, 0). \quad (\text{A7})$$

The diagonal components of the stress tensor  $\tau$  are given as

$$\tau_{rr} = -\frac{\dot{\epsilon}}{2} [\alpha_4 + (\alpha_1 + \alpha_5 + \alpha_6) n_r^2] \quad (\text{A8 } a)$$

$$\tau_{\theta\theta} = -\frac{\dot{\epsilon}}{2} [\alpha_4 + (\alpha_1 + \alpha_5 + \alpha_6) n_\theta^2] \quad (\text{A8 } b)$$

$$\tau_{zz} = \alpha_4 \dot{\epsilon}. \quad (\text{A8 } c)$$

Clearly  $\tau_{rr} \neq \tau_{\theta\theta}$ , therefore there are two distinct uniaxial extensional viscosities for discotic mesophases, given by:

$$\eta_{zr, \text{uni, disks}} = \frac{3}{2} \alpha_4 + \frac{1}{2} (\alpha_1 + \alpha_5 + \alpha_6) n_r^2 \quad (\text{A9 } a)$$

$$\eta_{z\theta, \text{uni, disks}} = \frac{3}{2} \alpha_4 + \frac{1}{2} (\alpha_1 + \alpha_5 + \alpha_6) n_\theta^2 \quad (\text{A9 } b)$$

Thus to characterize completely the extensional rheological properties of discotic mesophases, both viscosities need to be specified. As the extensional viscosities of discotic mesophases are microstructure dependent, see equations (A9 *a, b*), they can be directly related to the transverse fibre textures. For the ideal radial texture,  $\mathbf{n}_{ss} = (0, 1, 0)$ :

$$\eta_{zr, \text{uni, disks}}^r = \frac{3}{2} \alpha_4 \quad (\text{A10 } a)$$

$$\begin{aligned} \eta_{z\theta, \text{uni, disks}}^r &= \frac{3}{2} \alpha_4 + \frac{1}{2} (\alpha_1 + \alpha_5 + \alpha_6) \\ &= \frac{3}{2} \alpha_4 + \frac{1}{2} (\alpha_1 + \alpha_2 + \alpha_3 + 2\alpha_6) \end{aligned} \quad (\text{A10 } b)$$

For the ideal onion texture,  $\mathbf{n}_{ss} = (1, 0, 0)$ :

$$\begin{aligned} \eta_{zr, \text{uni, disks}}^o &= \frac{3}{2} \alpha_4 + \frac{1}{2} (\alpha_1 + \alpha_5 + \alpha_6) \\ &= \frac{3}{2} \alpha_4 + \frac{1}{2} (\alpha_1 + \alpha_2 + \alpha_3 + 2\alpha_6) \end{aligned} \quad (\text{A11 } a)$$

$$\eta_{z\theta, \text{uni, disks}}^o = \frac{3}{2} \alpha_4 \quad (\text{A11 } b)$$

Comparing equations (A10 *a, b* and A11 *a, b*) we have:

$$\eta_{zr, \text{uni, disks}}^r = \eta_{z\theta, \text{uni, disks}}^o \quad (\text{A12})$$

$$\eta_{z\theta, \text{uni, disks}}^r = \eta_{zr, \text{uni, disks}}^o. \quad (\text{A13})$$

For discotic nematics,  $\alpha_2 > 0$ ,  $\alpha_3 > 0$  [20],  $\alpha_4 > 0$ ,  $\alpha_5 < 0$ ,  $\alpha_6 > 0$  [21]. Also from the value of  $\alpha_1$  approximated in [21] we have:

$$\alpha_1 + \alpha_2 + \alpha_3 + 2\alpha_6 > 0. \quad (\text{A14})$$

Hence we obtain the following ordering among the uniaxial extensional viscosities for discotic nematics:

$$\eta_{\dot{\epsilon}r, \text{uni, disks}}^r < \eta_{\dot{\epsilon}\theta \text{uni, disks}}^r \quad (\text{A15})$$

$$\eta_{\dot{\epsilon}r, \text{uni, disks}}^o > \eta_{\dot{\epsilon}\theta \text{uni, disks}}^o \quad (\text{A16})$$

**References**

[1] PEEBLES, L. H., 1994, in *Carbon Fibers: Formation, Structures and Properties*, (Boca Raton: CRC Press).

[2] EDIE, D. D., ROBINSON, K. E., FLEUROT, O., JONES, S. P., and FAIN, C. C., 1994, *Carbon*, **32**, 1045.

[3] MCHUGH, J. J., and EDIE, D. D., 1992, *Carbon '92*, p. 683.

[4] MCHUGH, J. J., and EDIE, D. D., 1995, *Liq. Cryst.*, **18**, 327.

[5] FLEUROT, O., and EDIE, D. D., 1997, *Carbon '97*.

[6] FATHOLAH, B., and WHITE, J. L., 1994, *J. Rheo.*, **38**, 1591.

[7] FATHOLAH, B., GOPALAKRISHNAN, M. K., and WHITE, J. L., 1992, *Carbon '92*, p. 36.

[8] SINGH, A. P., and REY, A. D., 1995, *J. Phys. II Fr.*, **5**, 1321.

[9] SINGH, A. P., and REY, A. D., 1994, *J. Phys. II Fr.*, **4**, 645.

[10] SINGH, A. P., and REY, A. D., 1995, *Liq. Cryst.*, **18**, 219.

[11] DOI, M., and EDWARDS, S. F., 1986, in *The Theory of Polymer Dynamics* (New York: Oxford University Press).

[12] SINGH, A. P., and REY, A. D., 1998, *Rheol. Acta*, **37**, 30.

[13] DEGENNE, P. G., and PROUST, J., 1993, in *The Physics of Liquid Crystals*, 2nd Edn (London: Oxford University Press).

[14] LARSON, R. G., 1996, *Rheol. Acta*, **35**, 150.

[15] TSUJI, T., and REY, A. D., 1997, *J.N.N.F.M.*, **73**, 127.

[16] SINGH, A. P., and REY, A. D., 1998, *Rheol. Acta*, **37**, 374.

[17] DEALY, J. M., 1994, *J. Rheol.*, **38**, 179.

[18] REY, A. D., 1997, *Polym. Compos.*, **18**, 687.

[19] LESLIE, F. M., 1979, *Theory of flow phenomena in liquid crystals*, in *Advances in Liquid Crystals* (New York: Academic Press), p. 1.

[20] VOLOVIK, G. E., 1980, *JETP Lett.*, **31**, 273.

[21] MCHUGH, J. J., 1994, PhD. thesis, Clemson University, USA.